INSTITUTE OF PHYSICS PUBLISHING SMART MATERIALS AND STRUCTURES
Smart Mater. Struct. 10 (2001) 624–636 PII: S0964-1726(01)22816-X

Structural health monitoring by electrical resistance measurement

D D L Chung

Composite Materials Research Laboratory, State University of New York at Buffalo, Buffalo, NY 14260-4400, USA

Received 25 April 2000, in final form 10 January 2001
Published 18 July 2001
Online at stacks.iop.org/SMS/10/624

Abstract
Structural health monitoring by dc electrical resistance measurement is reviewed. The technique is valuable for evaluating composites and joints, provided that the materials involved are not all electrically insulating. The measurement pertains to either the volume electrical resistivity of a bulk material or the contact resistivity of an interface, and it can be performed in real time during loading or heating.

1. Introduction

Structural health monitoring refers to the monitoring of the integrity of a structure for the purpose of hazard mitigation, whether the hazard is due to live load, earthquake, wind, ocean waves, fatigue, aging, heat or other factors. This monitoring mainly entails non-destructive sensing of the damage in the structure.

Extensive damage, such as large cracks on the surface, can be sensed by visual inspection and liquid penetrant inspection. Both surface and sub-surface defects can be sensed by magnetic particle inspection (if the material is ferromagnetic), eddy current testing (if the material is electrically conducting and the defect is appropriately oriented with respect to the eddy current), ultrasonic testing (if the defect is appropriately oriented with respect to the ultrasonic wave propagation direction), x-radiography and other methods. However, these techniques tend to be not very sensitive to defects that are subtle in nature or microscopic in size. The resolution is particularly poor for magnetic particle inspection and x-radiography. The resolution tends to be better for ultrasonic methods, but it is still limited to about 0.1 mm (depending on the frequency of the ultrasonic wave). For effective hazard mitigation, it is important to be able to detect defects when they are small [1–7].

Recent attention on structural health monitoring has been centered on the use of embedded or attached sensors, such as piezoelectric, optical fiber, microelectromechanical, acoustic, dynamic response, phase transformation and other sensors [8–38], and the use of tagging through the incorporation of piezoelectric, magnetic or electrically conducting particles in the composite material [39, 40]. The use of embedded sensors or particles tends to suffer from the mechanical property degradation of the composite. Furthermore, embedded sensors are hard to repair. Attached sensors are easier to repair than embedded sensors, but they suffer from poor durability. Both embedded and attached sensors are much more expensive than the structural material, so they add much to the cost of the structure.

Electrical resistance measurement is a method which has received relatively little attention in terms of structural health monitoring. It does not involve any embedment or attachment, so it does not suffer from the problems described earlier for embedded or attached sensors. Furthermore, the method allows the entire structure to be monitored, whereas the use of embedded or attached sensors tends to allow the structure to be monitored at selected positions only. The electrical resistance method is particularly effective for detecting small and subtle defects in composite materials and in joints. Composite materials, such as carbon fiber polymer-matrix composites, are lightweight structural composites that are important for aircraft, for which structural health monitoring is critical. Joints, whether by fastening or adhesion, are encountered in almost any structure, and their structural health monitoring is particularly challenging, due to the difficulty of probing the joint interface. This paper reviews the electrical resistance (dc) method of structural health monitoring.

2. Carbon fiber polymer-matrix structural composites

Polymer-matrix composites for structural applications typically contain continuous fibers such as carbon, polymer and glass fibers, as continuous fibers tend to be more effective than short fibers as a reinforcement. Polymer-matrix composites with continuous carbon fibers are used for aerospace, automobile and civil structures. Due to the fact that carbon fibers are electrically conducting, whereas polymer and glass fibers are

not, carbon fiber composites exhibit electrical properties which depend on parameters such as damage, thereby attaining the ability to sense themselves through electrical measurement.

Within a lamina with tows in the same direction, the electrical conductivity is highest in the carbon fiber direction. In the transverse direction in the plane of the lamina, the conductivity is not zero, even though the polymer matrix is insulating, because there are contacts between fibers of adjacent tows [41]. In other words, a fraction of the fibers of one tow touches a fraction of the fibers of an adjacent tow here and there along the length of the fibers. These contacts result from the fact that fibers are not perfectly straight or parallel (even though the lamina is said to be unidirectional), and that the flow of the polymer matrix (or resin) during composite fabrication can cause a fiber to be not completely covered by the polymer or resin (even though, prior to composite fabrication, each fiber may be completely covered by the polymer or resin, as in the case of a prepreg, i.e. a fiber sheet impregnated with the polymer or resin). Fiber waviness is known as marcelling. Thus, the transverse conductivity gives information on the number of fiber–fiber contacts in the plane of the lamina.

For similar reasons, the contacts between fibers of adjacent laminae cause the conductivity in the through-thickness direction (direction perpendicular to the plane of the laminate) to be non-zero. Thus, the through-thickness conductivity gives information on the number of fiber–fiber contacts between adjacent laminae.

Matrix cracking between the tows of a lamina decreases the number of fiber–fiber contacts in the plane of the lamina, thus decreasing the transverse conductivity. Similarly, matrix cracking between adjacent laminae (as in delamination [42]) decreases the number of fiber–fiber contacts between adjacent laminae, thus decreasing the through-thickness conductivity. This means that the transverse and through-thickness conductivities can indicate damage in the form of matrix cracking.

Fiber damage (defect generation in the fiber, as distinct from fiber fracture) decreases the conductivity of a fiber, thereby decreasing the longitudinal conductivity (conductivity in the fiber direction). However, due to the brittleness of carbon fibers, the decrease in conductivity due to fiber damage prior to fiber fracture is rather small [43, 44].

Fiber fracture causes a much larger decrease in the longitudinal conductivity of a lamina than fiber damage. If there is only one fiber, a broken fiber results in an open circuit, i.e. zero conductivity. However, a lamina has a large number of fibers and adjacent fibers can make contact here and there. Therefore, the portions of a broken fiber still contribute to the longitudinal conductivity of the lamina. As a result, the decrease in conductivity due to fiber fracture is less than what it would be if a broken fiber did not contribute to the conductivity. Nevertheless, the effect of fiber fracture on the longitudinal conductivity is significant, so that the longitudinal conductivity can indicate damage in the form of fiber fracture [45].

The through-thickness volume resistance of a laminate is the sum of the volume resistance of each of the laminae in the through-thickness direction and the contact resistance of each of the interfaces between adjacent laminae (i.e. the interlaminar interface). For example, a laminate with

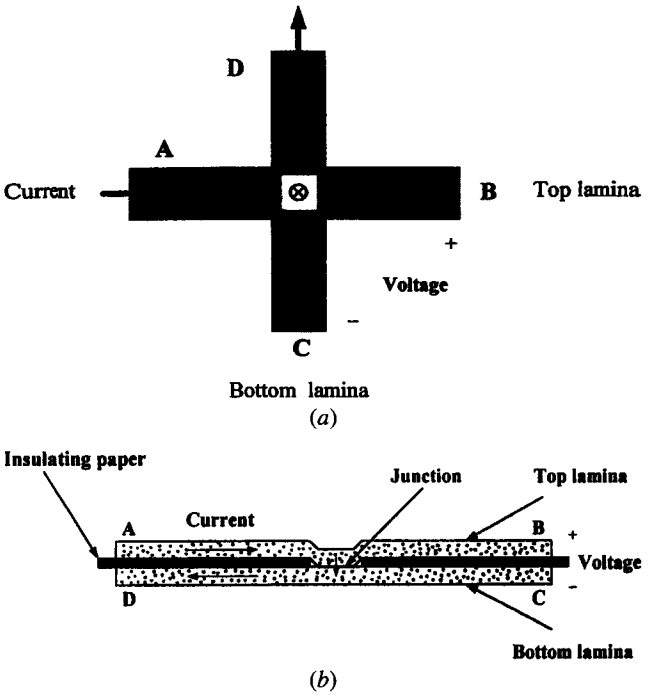

Figure 1. Specimen configuration for measurement of the contact electrical resistivity between laminae: (*a*) crossply laminae; (*b*) unidirectional laminae.

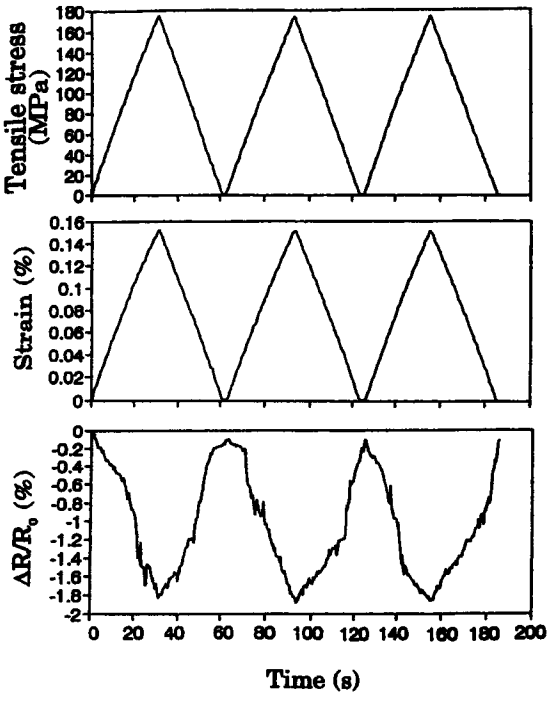

Figure 2. Longitudinal stress and strain and fractional resistance increase ($\Delta R/R_0$) obtained simultaneously during cyclic tension at a stress amplitude equal to 14% of the breaking stress for continuous fiber epoxy-matrix composite.

eight laminae has eight volume resistances and seven contact resistances, all in the through-thickness direction. Thus, to study the interlaminar interface, it is better to measure the contact resistance between two laminae rather than the through-thickness volume resistance of the entire laminate.

Measurement of the contact resistance between laminae can be made by allowing two laminae (strips) to contact at

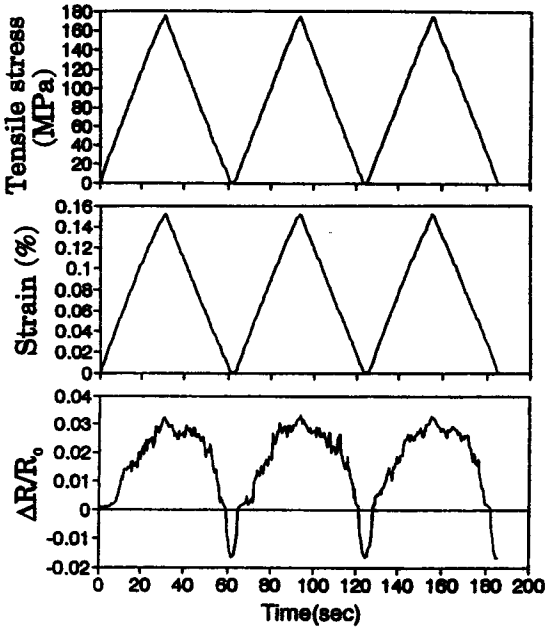

Figure 3. Longitudinal stress and strain and the through-thickness $\Delta R/R_0$ obtained simultaneously during cyclic tension at a stress amplitude equal to 14% of the breaking stress for continuous fiber epoxy-matrix composite.

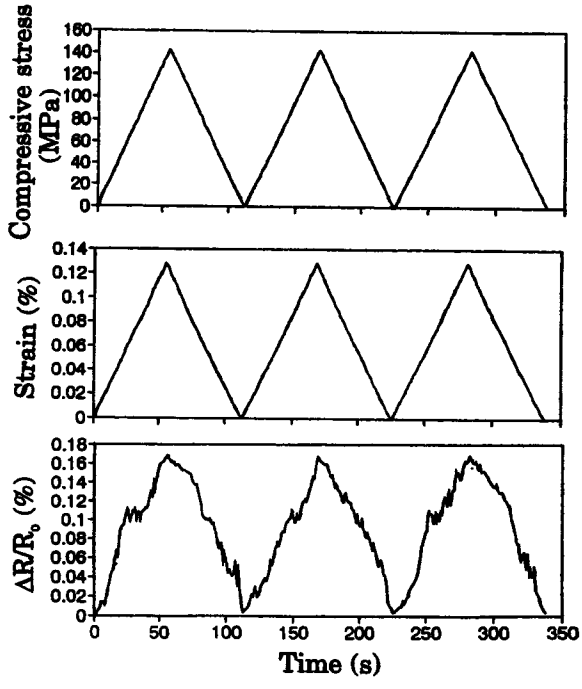

Figure 4. Longitudinal stress, strain and $\Delta R/R_0$ obtained simultaneously during cyclic compression (longitudinal) at a stress amplitude equal to 14% of the breaking stress for continuous fiber epoxy-matrix composite.

a junction and using the two ends of each strip for making four electrical contacts [46]. An end of the top strip and an end of the bottom strip serve as contacts for passing current. The other end of the top strip and the other end of the bottom strip serve as contacts for voltage measurement. The fibers in the two strips can be in the same direction or in different directions. This method is a form of the four-probe method of electrical resistance measurement. The configuration is illustrated in figure 1 for crossply and unidirectional laminates.

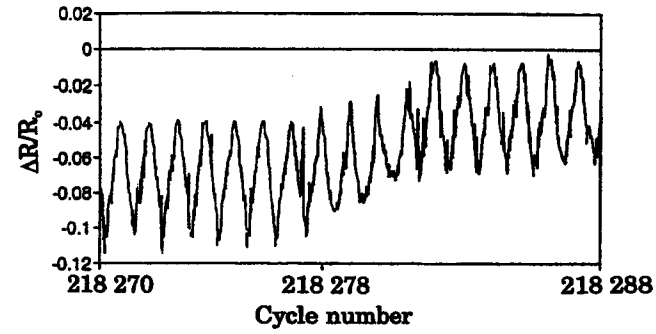

Figure 5. Variation of longitudinal $\Delta R/R_0$ with cycle number during tension–tension fatigue testing for a carbon fiber epoxy-matrix composite. Each cycle of reversible decrease in resistance is due to strain. The irreversible increase in resistance at around cycle no. 218 281 is due to damage in the form of fiber breakage.

To make sure that the volume resistance within a lamina in the through-thickness direction does not contribute to the measured resistance, the fibers at each end of a lamina strip should be electrically shorted together by using silver paint or other conducting media. The measured resistance is the contact resistance of the junction. This resistance, multiplied by the area of the junction, gives the contact resistivity, which is independent of the area of the junction and just depends on the nature of the interlaminar interface. The unit of the contact resistivity is $\Omega\,m^2$, whereas that of the volume resistivity is $\Omega\,m$.

The structure of the interlaminar interface tends to be more prone to change than the structure within a lamina. For example, damage in the form of delamination is much more common than damage in the form of fiber fracture. Moreover, the structure of the interlaminar interface (such as the extent of contact between fibers of adjacent laminae) is affected by the interlaminar stress (whether thermal stress or curing stress), which is particularly significant when the laminae are not unidirectional (as the anisotropy within each lamina enhances the interlaminar stress). The structure of the interlaminar interface also depends on the extent of consolidation of the laminae during composite fabrication. The contact resistance provides a sensitive probe of the structure of the interlaminar interface.

The measurement of the volume resistivity in the through-thickness direction can be conducted by using the four-probe method, in which each of the two current contacts is in the form of a conductor loop (made by silver paint, for example) on each of the two outer surfaces of the laminate in the plane of the laminate and each of the two voltage contacts is in the form of a conductor dot within the loop [42]. An alternative method is to have four of the laminae in the laminate be extra long so that they extend outwards for the purpose of serving as electrical leads [47]. The two outer leads are for current contacts; the two inner leads are for voltage contacts. The use of a thin metal wire inserted at an end into the interlaminar space during composite fabrication in order to serve as an electrical contact is not recommended, because the quality of the electrical contact between the metal wire and carbon fibers is hard to control and the wire is intrusive to the composite. The alternative method is less convenient than the method involving loops and dots, but it approaches more closely the ideal four-probe method.

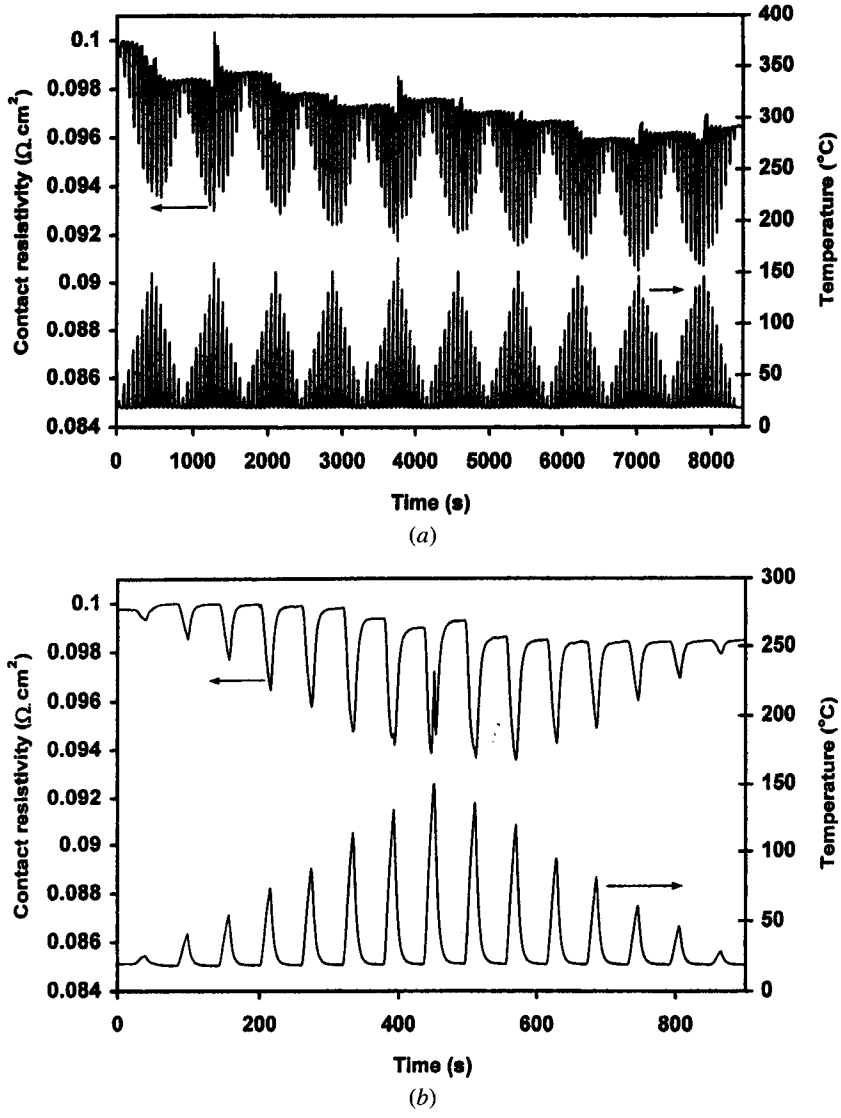

Figure 6. Variation of contact electrical resistivity with time and of the temperature with time during thermal cycling of a carbon fiber epoxy-matrix composite. (*b*) is the magnified view of the first 900 s of (*a*).

The simultaneous monitoring of damage (irreversible, whether due to stress or temperature, under static or dynamic conditions) and strain (reversible, due to stress under a dynamic condition) has been achieved in continuous carbon fiber polymer-matrix composites, as the electrical resistance of the composite changes with damage and strain [42, 48–62]. Upon longitudinal tension, the longitudinal resistivity decreases quite reversibly (figure 2), due to the increase in the degree of fiber alignment, while the through-thickness resistivity increases quite reversibly (figure 3) for the same reason. Upon longitudinal compression, the longitudinal resistivity increases quite reversibly (figure 4), due to decrease in the degree of fiber alignment. These essentially reversible effects of strain provide mechanisms for sensing strain. On the other hand, minor damage in the form of slight matrix damage and/or disturbance to the fiber arrangement is indicated by the longitudinal and through-thickness resistance decreasing irreversibly due to the increase in the number of contacts between fibers, as shown after one loading cycle in figures 2 and 3. The irreversible decrease after one cycle is slight in figure 2 and more significant in figure 3. More significant damage in the form of delamination or interlaminar interface degradation is indicated by the through-thickness resistance (or, more exactly, the contact resistivity of the interlaminar interface) increasing irreversibly (figure 5 for the case of damage during fatigue) due to the decrease in the number of contacts between fibers of different laminae. Major damage in the form of fiber breakage is indicated by the longitudinal resistance increasing irreversibly (not shown in the figures in this review), as supported by the accompanying decrease in modulus [49].

During mechanical fatigue (tension–tension fatigue, with stress in the longitudinal direction), delamination was observed to begin at 30% of the fatigue life, whereas fiber breakage was observed to begin at 50% of the fatigue life. Figure 5 [49] shows an irreversible resistance increase occurring at about 50% of the fatigue life during tension–tension fatigue testing of a unidirectional continuous carbon fiber epoxy-matrix composite. The resistance and stress are in the fiber direction. The reversible changes in resistance are due to elastic strain, which causes the resistance to decrease reversibly in each cycle, as in figure 2.

Figure 6 [50] shows the variation of the contact resistivity with temperature during thermal cycling. The temperature

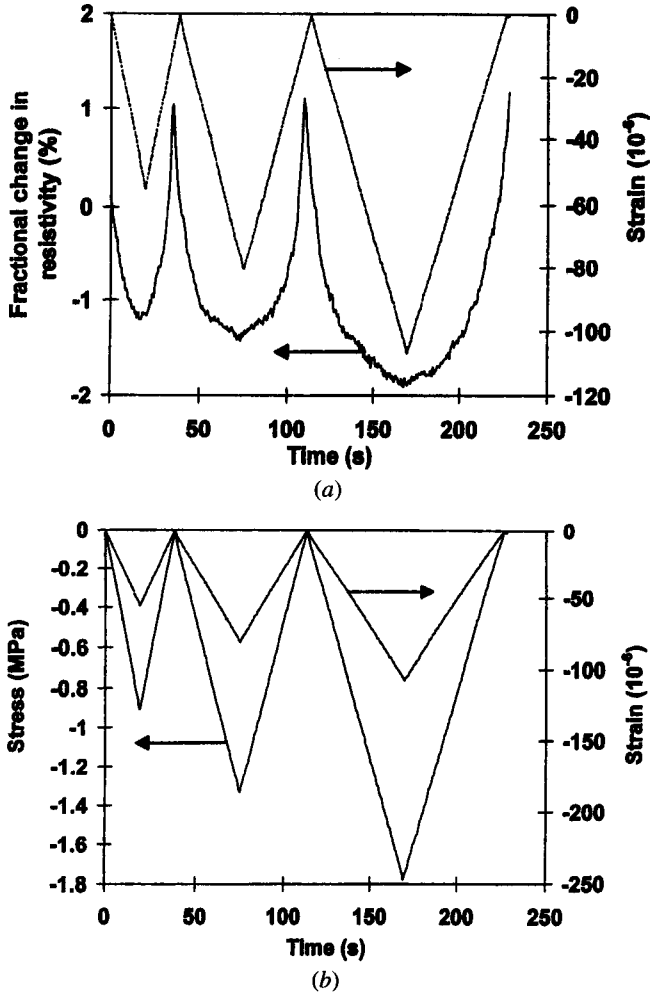

Figure 7. Variation of the fractional change in volume electrical resistivity with time (*a*), of the stress with time (*b*), and of the strain (negative for compressive strain) with time (*a*) and (*b*) during dynamic compressive loading at increasing stress amplitudes within the elastic regime for carbon-fiber latex cement paste at 28 days of curing.

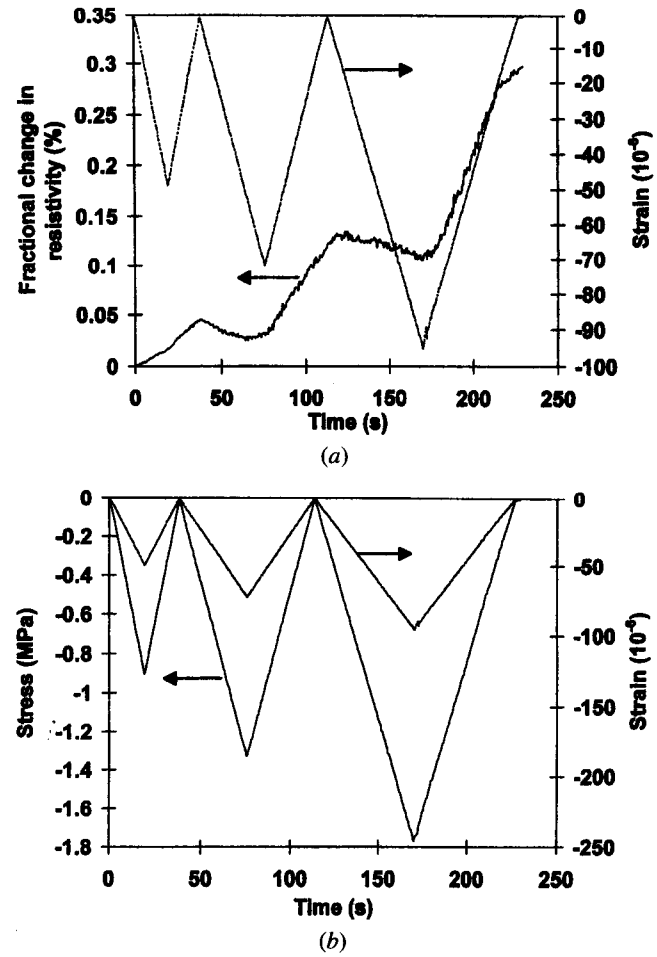

Figure 8. Variation of the fractional change in electrical resistivity with time (*a*), of the stress with time (*b*), and of the strain (negative for compressive strain) with time (*a*) and (*b*) during dynamic compressive loading at increasing stress amplitudes within the elastic regime for silica-fume cement paste at 28 days of curing.

is repeatedly increased to various levels. A group of cycles in which the temperature amplitude increases cycle by cycle and then decreases cycle by cycle back to the initial low-temperature amplitude is referred to as a group. Figure 6(*a*) shows the results of the first ten groups, while figure 6(*b*) shows the first group only. The contact resistivity decreases upon heating in every cycle of every group. At the highest temperature (150 °C) of a group, a spike of resistivity increase occurs, as shown in figure 6(*b*). It is attributed to thermal damage at the interlaminar interface, as the damage affects the extent of contact between fibers of adjacent laminae. In addition, the baseline resistivity (i.e. the top envelope) gradually and irreversibly shifts downward as cycling progresses, as shown in figure 6(*a*). The baseline decrease is probably due to matrix damage within a lamina and the resulting decrease in modulus and hence decrease in residual stress.

3. Cement-matrix composites

Concrete (a cement-matrix composite) is the dominant structural material for the civil infrastructure. Figure 7(*a*) shows the fractional change in resistivity along the stress direction as well as the strain during repeated compressive loading at an increasing stress amplitude for carbon-fiber (short fibers, at a volume fraction below the percolation threshold) latex cement paste at 28 days of curing. Figure 7(*b*) shows the corresponding variation of stress and strain during the repeated loading. The strain varies linearly with the stress up to the highest stress amplitude (figure 7(*b*)). The strain returns to zero at the end of each cycle of loading. The resistivity decreases upon loading in every cycle (due to fiber push-in) and increases upon unloading in every cycle (due to fiber pull-out), thereby allowing strain sensing [63–65]. The resistivity has a net increase after the first cycle, probably due to damage associated with the fiber-matrix interface. Little further damage occurs in subsequent cycles, as shown by the resistivity after unloading not increasing much after the first cycle. The greater the strain amplitude, the more is the resistivity decrease during loading, although the resistivity and strain are not linearly related. The effects of figure 7 were similarly observed in carbon-fiber silica-fume cement paste at 28 days of curing.

Concrete, particularly when short carbon fibers are present, is capable of sensing damage due to the electrical resistivity increase that accompanies damage [63–67]. That both strain and damage can be sensed simultaneously through

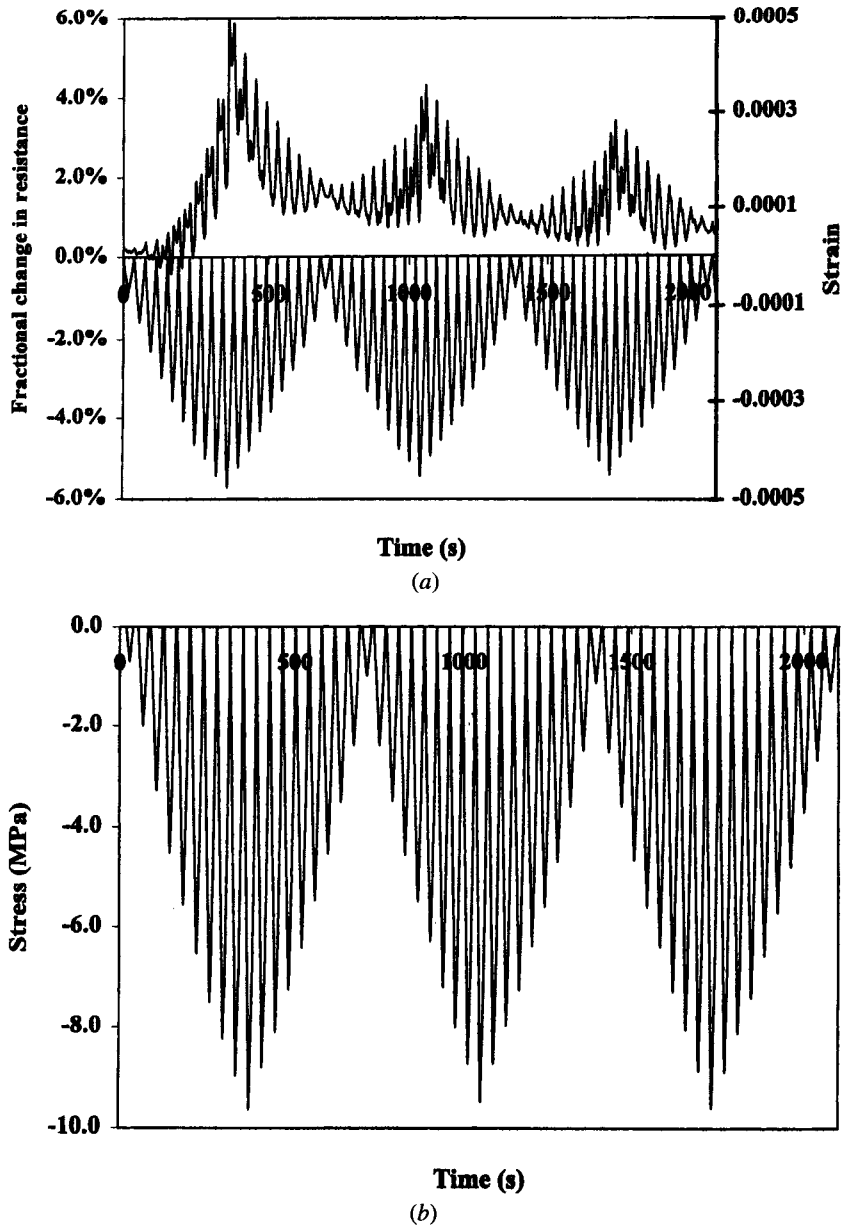

Figure 9. Fractional change in resistance (*a*), strain (*a*) and stress (*b*) during repeated compressive loading at increasing and decreasing stress amplitudes, the highest of which was 60% of the compressive strength, for carbon-fiber concrete at 28 days of curing.

resistance measurement means that the strain/stress condition (during dynamic loading) under which damage occurs can be obtained, thus facilitating damage origin identification. Damage is indicated by a resistance increase, which is larger and less reversible when the stress amplitude is higher. The resistance increase can be a sudden increase during loading. It can also be a gradual shift of the baseline resistance.

Figure 8(*a*) [66] shows the fractional change in resistivity along the stress direction as well as the strain during repeated compressive loading at an increasing stress amplitude for plain cement paste at 28 days of curing. Figure 8(*b*) shows the corresponding variation of stress and strain during the repeated loading. The strain varies linearly with the stress up to the highest stress amplitude (figure 8(*b*)). The strain returns to zero at the end of each cycle of loading. During the first loading, the resistivity increases due to damage initiation. During the subsequent unloading, the resistivity continues to increase, probably due to opening of the microcracks generated during loading. During the second loading, the resistivity decreases slightly as the stress increases up to the maximum stress of the first cycle (probably due to closing of the microcracks) and then increases as the stress increases beyond this value (probably due to the generation of additional microcracks). During unloading in the second cycle, the resistivity increases significantly (probably due to opening of the microcracks). During the third loading, the resistivity essentially does not change (or decreases very slightly) as the stress increases to the maximum stress of the third cycle (probably due to the balance between microcrack generation and microcrack closing). Subsequent unloading causes the resistivity to increase very significantly (probably due to opening of the microcracks).

Figure 9 shows the fractional change in resistance, strain and stress during repeated compressive loading at increasing and decreasing stress amplitudes for carbon fiber (0.18 vol.%) concrete (with fine and coarse aggregates) at 28 days of

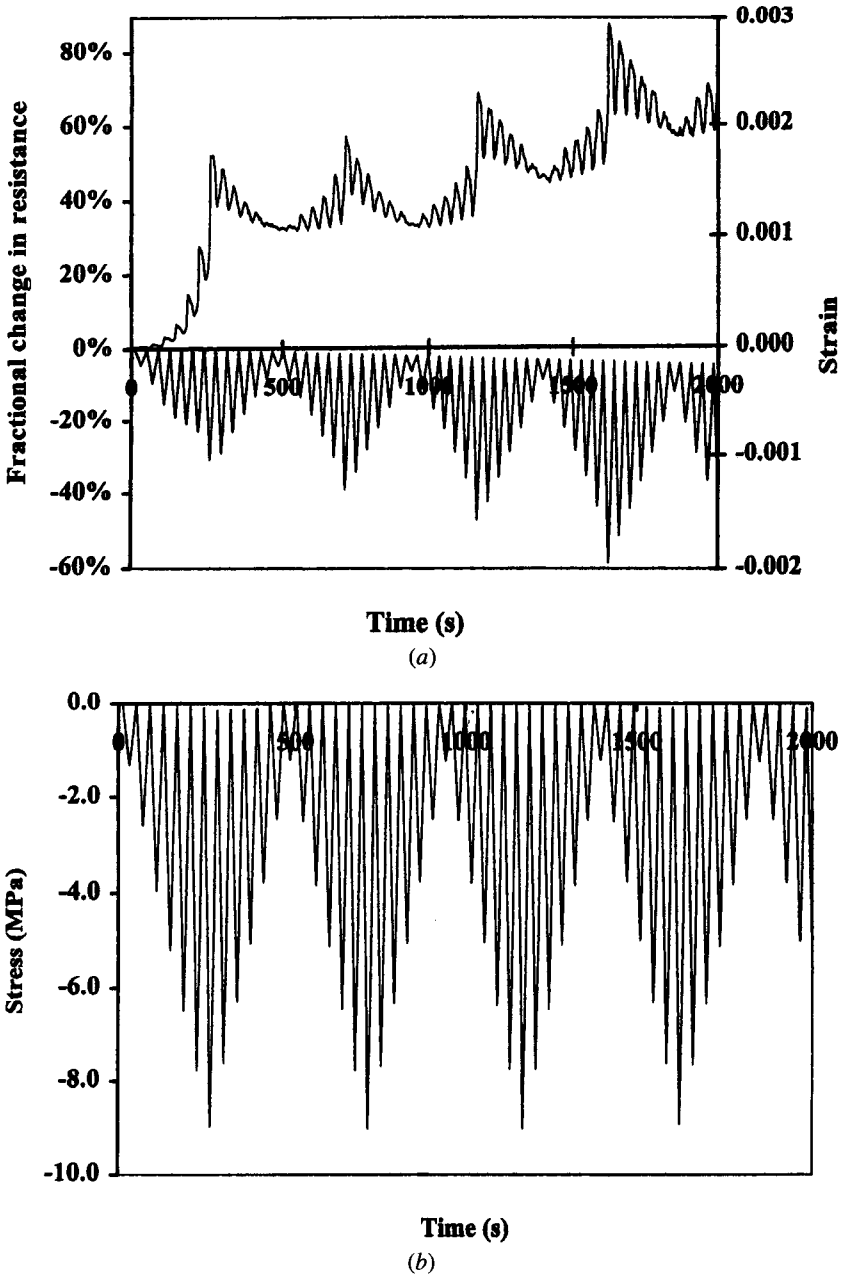

Figure 10. Fractional change in resistance (*a*), strain (*a*) and stress (*b*) during repeated compressive loading at increasing and decreasing stress amplitudes, the highest of which was greater than 90% of the compressive strength, for carbon-fiber concrete at 28 days of curing.

curing. The highest stress amplitude is 60% of the compressive strength. A group of cycles in which the stress amplitude increases cycle by cycle and then decreases cycle by cycle back to the initial low stress amplitude is hereby referred to as a group. Figure 9 shows the results for three groups. The strain returns to zero at the end of each cycle for any of the stress amplitudes, indicating elastic behavior. The resistance decreases upon loading in each cycle, as in figure 7. An extra peak at the maximum stress of a cycle grows as the stress amplitude increases, resulting in two peaks per cycle. The original peak (strain induced) occurs at zero stress, while the extra peak (damage induced) occurs at the maximum stress. Hence, during loading from zero stress within a cycle, the resistance drops and then increases sharply, reaching the maximum resistance of the extra peak at the maximum stress of the cycle. Upon subsequent unloading, the resistance decreases and then increases as unloading continues, reaching the maximum resistance of the original peak at zero stress. In the part of this group where the stress amplitude decreases cycle by cycle, the extra peak diminishes and disappears, leaving the original peak as the sole peak. In the part of the second group where the stress amplitude increases cycle by cycle, the original peak (peak at zero stress) is the only peak, except that the extra peak (peak at the maximum stress) returns in a minor way (more minor than in the first group) as the stress amplitude increases. The additional peak grows as the stress amplitude increases, but, in the part of the second group in which the stress amplitude decreases cycle by cycle, it quickly diminishes and vanishes, as in the first group. Within each group, the amplitude of resistance variation increases as the stress amplitude increases and decreases as the stress amplitude subsequently decreases.

The greater the stress amplitude, the larger and the less reversible is the damage-induced resistance increase (the extra

peak). If the stress amplitude has been experienced before, the damage-induced resistance increase (the extra peak) is small, as shown by comparing the result of the second group with that of the first group (figure 9), unless the extent of damage is large (figure 10 for a highest stress amplitude of greater than 90% the compressive strength). When the damage is extensive (as shown by a modulus decrease), damage-induced resistance increase occurs in every cycle, even at a decreasing stress amplitude, and it can overshadow the strain-induced resistance decrease (figure 10). Hence, the damage-induced resistance increase occurs mainly during loading (even within the elastic regime), particularly at a stress above that in prior cycles, unless the stress amplitude is high and/or damage is extensive.

At a high stress amplitude, the damage-induced resistance increases cycle by cycle as the stress amplitude increases causes the baseline resistance to increase irreversibly (figure 10). The baseline resistance in the regime of major damage (with a decrease in modulus) provides a measure of the extent of damage (i.e. condition monitoring). This measure works in the loaded or unloaded state. In contrast, the measure using the damage-induced resistance increase (figure 9) works only during stress increase and indicates the occurrence of damage (whether minor or major) as well as the extent of damage.

4. Joints

Joining is one of the key processes in manufacturing and repair. It can be achieved by welding, diffusion bonding (autohesion in the case of polymers), soldering, brazing, adhesion, fastening, or other methods.

Joints can be evaluated destructively by mechanical testing which involves debonding. However, it is preferred to use non-destructive methods, such as modulus (dynamic mechanical), acoustic and electrical measurements. Electrical measurements are particularly attractive, due to the short response time and equipment simplicity. A requirement for the feasibility of electrical measurements for joint evaluation is that the components being joined are not electrical insulators. Thus, joints involving metals, cement (concrete) and conductor filled polymers are suitable.

The method of electrical resistance measurement for joint evaluation most commonly involves measurement of the contact electrical resistivity of the joint interface. The contact resistivity is given by the product of the contact resistance and the joint area; it is a quantity that is independent of the joint area. Degradation of the joint causes the contact resistivity to increase. A less common method involves measuring the apparent volume resistance of a component while the component (A) is joined to another component (B). When component B is less conducting than component A, but is not insulating, degradation of the joint causes the apparent volume resistance of component A to increase. Both of these methods are illustrated below.

4.1. Joints involving composite and concrete by adhesion

Continuous fiber polymer-matrix composites are increasingly used to retrofit concrete structures, particularly columns [68–70]. The retrofit involves wrapping a fiber sheet around a concrete column or placing a sheet on the surface of a concrete structure, such that the fiber sheet is adhered to the underlying concrete by using a polymer, most commonly epoxy. This method is effective for the repair of even quite badly damaged concrete structures. Although the fibers and polymer are very expensive compared to concrete, the alternative of tearing down and rebuilding the concrete structure is often even more expensive than the composite retrofit. Both glass fibers and carbon fibers are used for the composite retrofit. Glass fibers are advantageous for their relatively low cost, but carbon fibers are advantageous for their high tensile modulus.

The effectiveness of a composite retrofit depends on the quality of the bond between the composite and the underlying concrete, as good bonding is necessary for load transfer. Peel testing for bond quality evaluation is destructive [71]. Non-destructive methods to evaluate the bond quality are valuable. They include acoustic methods, which are not sensitive to small amounts of debonding or bond degradation [72], and dynamic mechanical testing [73]. Electrical resistance measurement was used for non-destructive evaluation of the interface between concrete and its carbon fiber composite retrofit [68]. The method is effective for studying the effects of temperature and debonding stress on the interface. The concept behind the method is that bond degradation causes the electrical contact between the carbon fiber composite retrofit and the underlying concrete to degrade. Since concrete is electrically more conducting than air, the presence of an air pocket at the interface causes the measured apparent volume resistance of the composite retrofit in a direction in the plane of the interface to increase. Hence, bond degradation is accompanied by an increase in the apparent resistance of the composite retrofit. Although the polymer matrix (epoxy) is electrically insulating, the presence of a thin layer of epoxy at the interface is unable to electrically isolate the composite retrofit from the underlying concrete.

The apparent resistance of the retrofit in the fiber direction is increased by bond degradation, whether the degradation is due to heat or stress. The degradation is reversible. Irreversible disturbance in the fiber arrangement occurs slightly as thermal or load cycling occurs, as indicated by the resistance decreasing cycle by cycle [68].

4.2. Joints involving composites by adhesion

Joining methods for polymers and polymer-matrix composites include autohesion, which is relevant to the self-healing of polymers. Diffusion bonding (or autohesion) involves interdiffusion between the adjoining materials in the solid state. In contrast, fusion bonding involves melting. Due to the relatively low temperatures of diffusion bonding compared to fusion bonding, diffusion bonding does not suffer from the undesirable side effects that typically occur in fusion bonding, such as degradation and crosslinking of the polymer matrix. Although the diffusion bonding of metals has been widely studied, relatively little study has been conducted on the autohesion of polymers. Because of the increased segment mobility above the glass transition temperature (T_g), thermoplastics are able to undergo interdiffusion above T_g.

Diffusion, as a thermally activated process, takes time. In other words, how long diffusion takes depends on the

temperature. In order for diffusion bonding or autohesion to be conducted properly, the kinetics of the process needs to be known.

The study of the kinetics requires monitoring the process as it occurs. A real-time monitoring technique is obviously preferable to a traditional method that requires periodic interruption and cooling of the specimen. However, real-time monitoring is experimentally difficult compared with interrupted monitoring. The method described here is ideal for thermoplastic prepregs containing continuous carbon fibers, since the carbon fibers are conductive. Two carbon-fiber thermoplastic prepreg plies are placed together to form a joint. The electrical contact resistance of this joint is measured during autohesion. As autohesion occurs, the fibers in the plies undergoing joining come closer together, thus resulting in a decrease in the contact resistance. Hence, with the measurement of this resistance in real time, the autohesion process was monitored as a function of time at different selected bonding temperatures for Nylon-6 and polyphenylenesulfide (PPS), both thermoplastics [74]. Arrhenius plots of a characteristic resistance decrease versus temperature allow determination of the activation energy for the process. This method can possibly be used for monitoring of bonding of unfilled thermoplastics if a few carbon fibers are strategically placed.

Engineering thermoplastics can be bonded together by autohesion above the glass transition temperature but below the melting temperature, or fusion welding (i.e. melting and subsequent solidification). Both methods involve heating and subsequent cooling. During cooling, the thermoplastic goes from a soft solid state (in the case of autohesion) or a liquid state (in the case of fusion welding) to a stiff state. If the thermoplastic members to be joined are anisotropic (as in the case of each member being reinforced with fibers) and the fiber orientation in the two members is not the same, the thermal expansion (actually contraction) mismatch at the bonding plane will cause thermal stress to build up during cooling. This thermal stress is detrimental to the quality of the adhesive bond formed between the two members.

Two scenarios can lead to the absence of bonding after cooling. One scenario is the absence of bond formation at the high temperature during welding, due to insufficient time or temperature. The other scenario is the presence of bonding at the high temperature, but the occurrence of debonding during subsequent cooling due to thermal stress. The cause of the absence of bonding is different in the two scenarios. In any given situation, the cause of the debonded joint must be understood if the absence of bonding after cooling is to be avoided.

The propensity for mutual diffusion in thermoplastic polymers increases with temperature. The contact at the interface across which interdiffusion takes place also plays a role. An intimate interface, as obtained by application of pressure to compress the two members together, also facilitates diffusion. Thus, the quality of the joint improves with increasing temperature and increasing pressure in the high-temperature period of welding. The poorer the quality of the joint attained at a high temperature is, the greater is the likelihood that thermal stress built up during subsequent cooling will be sufficient to cause debonding. Hence, merely having bonding achieved at the high temperature in welding is not enough. The bond achieved must be of sufficient quality to withstand the abuse of thermal stress during subsequent cooling.

The quality of a joint is conventionally tested destructively by mechanical methods or non-destructively by ultrasonic methods [75,76]. This testing is performed at room temperature after the joint has been cooled from the high temperature used in welding. As a result, the testing does not allow distinction between the two scenarios previously described. The use of a non-destructive method, namely contact electrical resistance measurement, to monitor joint quality in real time during the high-temperature period of welding and also during subsequent cooling has been shown [77]. The resistance increases by up to 600% upon debonding. The resistance increase is much greater than the resistance decrease during prior bonding. Debonding occurs during cooling when the pressure or temperature during prior bonding is not sufficiently high.

The adhesive joint formation between thermoplastic adherends typically involves heating to temperatures above the melting temperature (T_m) of the thermoplastic. During heating to the desired elevated temperature, time is spent in the range between the glass transition temperature (T_g) and T_m. The dependence of the bond quality on the heating rate, heating time, and pressure was investigated through measurement of the contact resistance between adherends in the form of carbon-fiber-reinforced PPS [78]. A long heating time below the melting temperature (T_m) is detrimental to subsequent PPS adhesive joint development above T_m. This is due to curing reactions below T_m and consequent reduced mass flow response above T_m. A high heating rate (small heating time) enhances the bonding more than a high pressure.

4.3. Joints involving steels by fastening

Mechanical fastening involves the application of a force to the components to be joined, so as to prevent the components from separating in service. During repair, maintenance or other operations, unfastening may be needed. Hence, repeated fastening and unfastening may be necessary. By design, the stresses encountered by the components and fasteners are below the corresponding yield stresses, so that no plastic deformation occurs. However, the local stress at the asperities at the interface can exceed the yield stress, thereby resulting in local plastic deformation, as shown for carbon steel fastened joints at a compressive stress of just 7% or less of the yield stress [79]. The plastic deformation results in changes in the joint interfaces. This means that the joint interface depends on the extent of prior fastening and unfastening. The joint interface affects the mechanical and corrosion behavior of the joint. This problem is thus of practical importance.

Stainless steel differs from carbon steel in the presence of a passive film, which is important to the corrosion resistance of stainless steel. The effect of repeated fastening and unfastening on the passive film is of concern.

Figure 11 [80] shows the variation in resistance and displacement during cyclic compressive loading of stainless steel on stainless steel at a stress amplitude of 14 MPa. In every cycle, the resistance decreases as the compressive stress

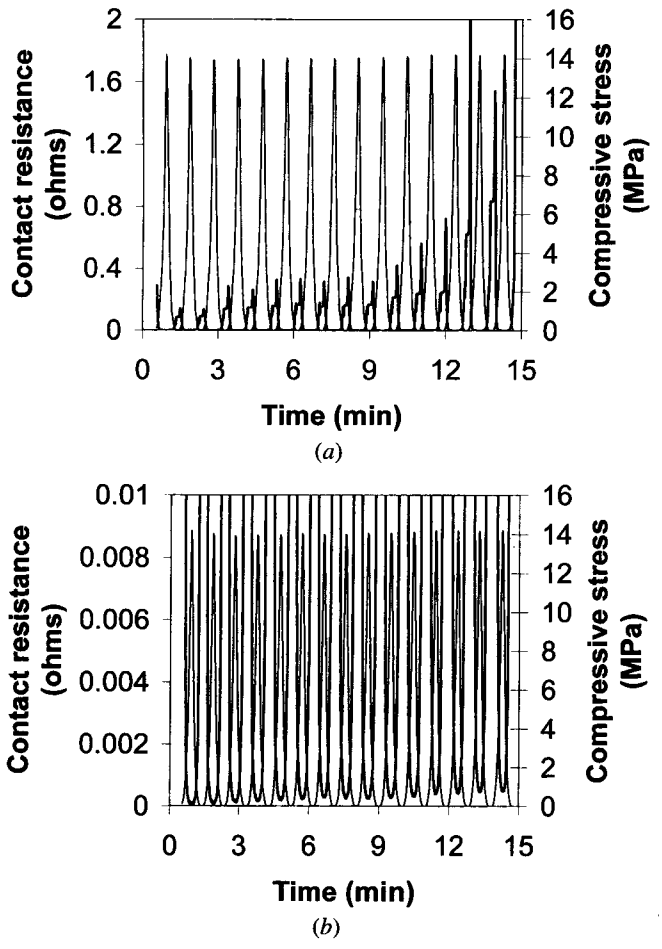

Figure 11. Variation of contact resistance (thick curve) and stress (thin curve) during cyclic compression of stainless steel on stainless steel at a stress amplitude of 14 MPa: (*a*) full-scale variation of resistance; (*b*) low resistance regime.

increases, such that the maximum stress corresponds to the minimum resistance and the minimum stress corresponds to the maximum resistance (figure 11(*a*)).

The maximum resistance (in the unloaded condition) of every cycle increases upon stress cycling, such that the increase is not significant until after 13 cycles (figure 11(*a*)). The increase is due to the damage of the passive film and the consequent surface oxidation. The minimum resistance (at the maximum stress) of every cycle increases slightly upon cycling (figure 11(*b*)), probably due to strain hardening.

The higher the stress amplitude is, the fewer is the number of stress cycles for passive film damage to start. At the lowest stress amplitude of 3.5 MPa, passive film damage was not observed up to 30 cycles.

Comparison of the results on stainless steel and on carbon steel shows that the carbon steel joint is dominated by effects associated with plastic deformation whereas the stainless steel joint is dominated by effects associated with passive film damage. The effect of the passive film is absent in the carbon steel joint, as expected from the absence of a passive film on carbon steel. The effects of plastic deformation and strain hardening at asperities are much larger for carbon steel than stainless steel, as expected from the lower yield stress of carbon steel.

4.4. Joints involving concrete by pressure application

Many concrete structures involve the direct contact of one cured concrete element with another, such that one element exerts static pressure on the other due to gravity. In addition, dynamic pressure may be exerted by live loads on the structure. An example of such a structure is a bridge involving slabs supported by columns, with dynamic live loads exerted by vehicles traveling on the bridge. Another example is a concrete floor in the form of slabs supported by columns, with live loads exerted by people walking on the floor. The interface between concrete elements that are in pressure contact is of interest, as it affects the integrity and reliability of the assembly. For example, deformation at the interface affects the interfacial structure, which can affect the effectiveness of load transfer between the contacting elements and can affect the durability of the interface to the environment. Moreover, deformation at the interface can affect the dimensional stability of the assembly. Of particular concern is how the interface is affected by dynamic loads.

A mortar–mortar contact has been studied under dynamic loading at different compressive stress amplitudes by measuring the contact electrical resistance [81, 82]. Irreversible decrease in the contact resistance upon unloading was observed as load cycling progressed at a low stress amplitude (5 MPa, compared to a value of 64 MPa for the compressive strength of the mortar), due to local plastic deformation at the asperities at the interface. Irreversible increase in the contact resistance at the maximum stress was observed as load cycling progressed, probably due to debris generation; it was more significant at a higher stress amplitude (15 MPa).

4.5. Joints involving composites by fastening

Fasteners as well as components are most commonly made of metals, such as steel. However, polymers are increasingly used for both fasteners and components, due to their moldability, low density and corrosion resistance.

Due to the electrically insulating behavior of conventional polymers and the need for an electrical conductor for the purpose of measuring the contact electrical resistance, a polymer that contained continuous carbon fibers in a direction parallel to the plane of the joint was used [83]. The carbon fibers cause the composite to be electrical conducting in the fiber direction, as well as the through-thickness direction, because there is some degree of contact between adjacent fibers in the composite in spite of the presence of the matrix [42]. Due to the direction of the fibers, the mechanical properties of the composite in the through-thickness direction is dominated by the polymer matrix.

Contact resistance measurement was used to investigate the effect of repeated fastening and unfastening on a composite–composite joint interface [83]. A composite–composite joint obtained by mechanical fastening at a compressive stress of 5% (or less) of the 1% offset yield strength of the polymer (Nylon-6) was found to exhibit irreversible decrease in the contact electrical resistance upon repeated fastening (loading) and unfastening (unloading). The decrease occurs after up to ten cycles of fastening and unfastening, although the decrease diminishes with cycling. It is primarily due to local plastic deformation of the matrix at

the asperities at the interface. Moreover, the stress required for the resistance to reach its minimum in a cycle decreases with cycling, due to softening of the matrix.

5. Conclusion

The measurement of dc electrical resistance is useful for structural health monitoring, particularly in relation to composites and joints, provided that the materials involved are not all electrically insulating. The monitoring involves measuring the volume resistivity of a bulk material or the contact resistivity of an interface. The measurement can be conducted in real time during loading or heating.

References

[1] Burke S K, Cousland S M and Scala C M 1994 Nondestructive characterization of advanced composite materials *Mater. Forum* **18** 85–109

[2] Achenbach J D 2000 Quantitative non-destructive evaluation *Int. J. Solids Struct.* **37** 13–27

[3] Rens K L, Wipf T J and Klaiber F W 1997 Review of non-destructive evaluation techniques of civil infrastructure *J. Perf. Constr. Facilities* **11** 152–60

[4] Heyman J S 1990 NDE research for aging aircraft integrity *Proc. IEEE* **2** 975–81

[5] Jiles D C 1988 Review of magnetic methods for non-destructive evaluation *NDT & E Int.* **21** 311–19

[6] Palanisamy R 1988 Remote-field eddy current testing: a review *Rev. Prog. Quantit. Nondestruct. Eval.* **7** 157–64

[7] Kinra V K and Dayal V 1987 Ultrasonic non-destructive evaluation of fibre-reinforced composite materials—a review *Sadhana* **11** 419–32

[8] Vipperman J S 1999 Novel autonomous structural health monitoring using piezoelectrics *AIAA/ASME/ASCE/AHS Conf. on Structures, Structural Dynamics & Materials, Technical Papers* vol 4, pp 3107–14

[9] Foedinger R C, Rea D L, Sirkis J S, Baldwin C S, Troll J R, Grande R, Davis C S and VanDiver T L 1999 Embedded fiber optic sensor arrays for structural health monitoring of filament wound composite pressure vessels *Proc. SPIE* **3670** 289–301

[10] Deng X, Wang Q and Giurgiutiu V 1999 Structural health monitoring using active sensors and wavelet transforms *Proc. SPIE* **3668** 363–70

[11] Jiang Z, Kabeya K and Chonan S 1999 Longitudinal wave propagation measuring technique for structural health monitoring *Proc. SPIE* **3668** 343–50

[12] Boller C, Biemans C, Staszewski W J, Worden K and Tomlinson G R 1999 Structural damage monitoring based on an actuator-sensor system *Proc. SPIE* **3668** 285–94

[13] Castillo D M, Pardo de Vera C and Guemes J A 1999 Structural integrity analysis with piezoelectric patches *Key Eng. Mater.* **167** 91–101

[14] Wang Q and Deng X 1999 Damage detection with spatial wavelets *Int. J. Solids Struct.* **36** 3443–68

[15] Pascual R, Golinval J C and Razeto M 1999 On-line damage assessment using operating deflection shapes *Proc. 17th Int. IMAC, SEM Conf. on Modal Analysis (Bethel, CT, 1999)* vol 1 pp 238–43

[16] Maclean B J, Mladejovsky M G, Whitaker M R, Olivier M and Jacobsen S C 1998 Digital MEMS-based strain gage for structural health monitoring *Proc. MRS Symp. on Nondestructive Characterization of Materials in Aging Systems* vol 503 (Warrendale, PA: Materials Research Society) pp 309–20

[17] Foedinger R, Rea D, Sirkis J, Wagreich R, Troll J, Grande R, Davis C and Vandiver T L 1998 Structural health monitoring of filament wound composite pressure vessels with embedded optical fiber sensors *Proc. 43rd Int. SAMPE Symp. and Exhibition (SAMPE, Covina, CA, 1998)* vol 43 pp 444–57

[18] Groves-Kirkby C J 1998 Optical-fibre strain sensing for structural health and load monitoring *GEC J. Technol.* **15** 16–26

[19] Beard S and Chang F-K 1997 Active damage detection in filament wound composite tubes using built-in sensors and actuators *J. Intell. Mater. Syst. Struct.* **8** 891–7

[20] Reich G W and Park K C 1998 Structural health monitoring via structural localization *AIAA/ASME/ASCE/AHS/ASC Conf. on Structures, Structural Dynamics and Materials, Technical Papers* vol 2 (Reston, VA: AIAA) pp 1653–60

[21] Polla D, Francis L, Robbins W and Harjani R 1997 MEMS for integrated diagnostic applications *Emerging Technologies for Machinery Health Monitoring and Prognosis* vol 7 (Fairfield, NJ: American Society of Mechanical Engineers, Tribology Division) pp 19–24

[22] Schulz M J, Naser A S, Thyagarajan S K, Mickens T and Pai P F 1998 Structural health monitoring using frequency response functions and sparse measurements *Proc. 16th Int. Conf. on IMAC. SEM Modal Analysis (Bethel, CT, 1998)* vol 1 pp 760–6

[23] James G H III, Zimmerman D C and Mayes R L 1998 Experimental study of frequency response function (FRF) based damage assessment tools *Proc. 16th Int. Conf. on IMAC. SEM Modal Analysis (Bethel, CT, 1998)* vol 1 pp 151–7

[24] Inaudi D, Casanova N, Kronenberg P, Marazzi S and Vurpillot S 1997 Embedded and surface-mounted fiber optic sensors for civil structural monitoring *Proc. SPIE* **3044** 236–43

[25] Ellerbrock P J 1997 DC-XA structural health-monitoring fiber optic-based strain measurement system *Proc. SPIE* **3044** 207–18

[26] Aktan A E, Helmicki A J, Hunt V J, Catbas N, Lenett M and Levi A 1997 Structural identification for condition assessment of civil infrastructure. *Proc. American Control Conf.* vol 2 (Piscataway, NJ: IEEE) pp 873–7

[27] Fells J A J, Goodwin M J, Groves-Kirkby C J, Reid D C J, Rule J E and Shell M B 1997 Fibre optic sensing for military bridge health and load monitoring *IEEE Coll. (Digest)* **33** 10/1–10/11

[28] Ballinger R S and Herrin D W 1995 Structural health monitoring using modal strain energy *Proc. 11th ASME Biennial Conf. on Reliability, Stress Analysis, and Failure Prevention* vol 83 (New York: American Society of Mechanical Engineers, Design Engineering Division) pp 181–7

[29] Zimmerman D C, Smith S W, Kim H M and Bartkowicz T J 1996 Experimental study of structural health monitoring using incomplete measurements *J. Vib. Acoustics* **118** 543–50

[30] Schoess J N, Seifert G and Paul C A 1996 Smart aircraft fastener evaluation (SAFE) system: a condition-based corrosion detection system for aging aircraft *Proc. SPIE* **2718** 175–84

[31] Schoess J N 1996 Rotor acoustic monitoring system (RAMS): a fatigue crack detection system *Proc. SPIE* **2717** 212–18

[32] Schoess J, Malver F, Iyer B and Kooyman J 1996 Rotor acoustic monitoring system (RAMS)—an application of acoustic emission integrity monitoring and assessment *Proc. 52nd Ann. Forum of American Helicopter Society (Alexandria, VA, 1996)* vol 2, pp 1788–93

[33] Castanien K E and Liang C 1996 Application of active structural health monitoring technique to aircraft fuselage structures *Proc. SPIE* **2721** 38–49

[34] James G, Roach D, Hansche B, Meza R and Robinson N 1996 Health monitoring studies on composite structures for aerospace applications *Proc. Int. Conf. on Engineering, Construction, and Operations in Space* vol 2 (New York: ASCE) pp 1127–33

[35] Westermo B D and Thompson L D 1995 Passive monitoring systems for structural damage assessment *Proc. SPIE* **2443** 841–51
[36] Zimmerman D C, Kaouk M and Simmermacher T 1995 Structural health monitoring using vibration measurements and engineering insight *J. Mech. Design* B **117** 214–21
[37] Narendran N and Weiss J 1995 High temperature fiber-optic strain and temperature sensor for structural health monitoring *Proc. Instrumentation, Control, and Automation in the Power Industry* vol 38 (Research Triangle Park, NC: Instrument Society of America) pp 273–82
[38] Sofge D A 1994 Structural health monitoring using neural network based vibrational system identification *Proc. 2nd Australian and New Zealand Conf. on Intelligent Information Systems* (Piscataway, NJ: IEEE) pp 91–4
[39] White S R 1995 Smart tagged composite using piezoelectric particles *Proc. SPIE* **2442** 337–48
[40] Quattrone R F and Berman J B 1996 Recent advancements in smart tagged composites for infrastructure *Materials for the New Millennium Proc. of Mater. Eng. Conf.* vol 2 (New York: ASCE) pp 1045–54
[41] Wang X and Chung D D L 1998 An electromechanical study of the transverse behavior of carbon fiber polymer-matrix composite *Comp. Interfaces* **5** 191–9
[42] Wang X and Chung D D L 1997 Sensing delamination in a carbon fiber polymer-matrix composite during fatigue by electrical resistance measurement *Polymer Comp.* **18** 692–700
[43] Wang X and Chung D D L 1997 Electromechanical behavior of carbon fiber *Carbon* **35** 706–9
[44] Wang X, Fu X and Chung D D L 1999 Strain sensing using carbon fiber. *J. Mater. Res.* **14** 790–802
[45] Wang X and Chung D D L 1999 Fiber breakage in polymer-matrix composite during static and dynamic loading, studied by electrical resistance measurement *J. Mater. Res.* **14** 4224–9
[46] Wang S and Chung D D L 1999 Interlaminar interface in carbon fiber polymer-matrix composites, studied by contact electrical resistivity measurment *Comp. Interfaces* **6** 497–506
[47] Wang S and Chung D D L 2000 Piezoresistivity in continuous carbon fiber polymer-matrix composite *Polymer Comp.* **21** 13–19
[48] Muto N, Yanagida H, Nakatsuji T, Sugita M, Ohtsuka Y and Arai Y 1992 Design of intelligent materials with self-diagnosing function for preventing fatal fracture *Smart Mater. Struct.* **1** 324–9
[49] Wang X, Wang S and Chung D D L 1999 Sensing damage in carbon fiber and its polymer-matrix and carbon-matrix composites by electrical resistance measurement *J. Mater. Sci.* **34** 2703–14
[50] Wang S and Chung D D L Thermal damage of carbon fiber polymer-matrix composite, monitored in real time by electrical resistivity measurement *Polymer Comp.* at press
[51] Muto N, Yanagida H, Miyayama M, Nakatsuji T, Sugita M and Ohtsuka Y 1992 Foreseeing of fracture in CFGFRP composites by the measurement of residual change in electrical resistance *J. Ceramic Soc. Japan* **100** 585–8
[52] Muto N, Yanagida H, Nakatsuji T, Sugita M, Ohtsuka Y, Arai Y and Saito C 1995 Materials design of CFGFRP-reinforced concretes with diagnosing function for preventing fatal fracture *Adv. Comp. Mater.* **4** 297–308
[53] Prabhakaran R 1990 Damage assessment through electrical resistance measurement in graphite fiber-reinforced composites *Exp. Techniques* **14** 16–20
[54] Sugita M, Yanagida H and Muto N 1995 Materials design for self-diagnosis of fracture in CFGFRP composite reinforcement *Smart Mater. Struct.* **4** A52–A57
[55] Kaddour A S, Al-Salehi F A R, Al-Hassani S T S and Hinton M J 1994 Electrical resistance measurement technique for detecting failure in CFRP materials at high strain rates *Comp. Sci. Technol.* **51** 377–85
[56] Ceysson O, Salvia M and Vincent L 1996 Damage mechanisms characterization of carbon fibre/epoxy composite laminates by both electrical resistance measurements and acoustic emission analysis *Scr. Mater.* **34** 1273–80
[57] Schulte K and Baron Ch 1989 Load and failure analyses of CFRP laminates by means of electrical resistivity measurements *Comp. Sci. Technol.* **36** 63–76
[58] Schulte K 1993 Damage monitoring in polymer matrix structures *J. Physique IV* C7 **3** 1629–36
[59] Abry J C, Bochard S, Chateauminois A Salvia M and Giraud G 1999 In situ detection of damage in CFRP laminates by electrical resistance measurements *Comp. Sci. Technol.* **59** 925–35
[60] Tedoroki A Kobayashi H and Matuura K 1995 Application of electric potential method to smart composite structures for detecting delamination *JSME Int. J.* A **38** 524–30.
[61] Hayes S, Brooks D, Liu T, Vickers S and Fernando G F 1996 In-situ self-sensing fibre reinforced composites *Proc. SPIE* **2718** 376–84
[62] Wang S and Chung D D L 1999 Apparent negative electrical resistance in carbon fiber composites *Composites* B **30** 579–90
[63] Chen P and Chung D D L 1993 Carbon fiber reinforced concrete as a smart material capable of non-destructive flaw detection *Smart Mater. Struct.* **2** 22–30
[64] Chen P and Chung D D L 1996 Carbon fiber reinforced concrete as an intrinsically smart concrete for damage assessment during static and dynamic loading *ACI Mater. J.* **93** 341–50
[65] Chung D D L 1995 Strain sensors based on the electrical resistance change accompanying the reversible pull-out of conducting short fibers in a less conducting matrix *Smart Mater. Struct.* **4** 59–61
[66] Bontea D, Chung D D L and Lee G C 2000 Damage in carbon fiber reinforced concrete, monitored by electrical resistance measurement *Cement Concrete Res.* **30** 651–9
[67] Lee J and Baston G 1996 Electrical tagging of fiber reinforced cement composite. Materials for the New Millennium *Proc. 4th Materials Engineering Conf.* vol 2 (New York: ASCE) pp 887–96
[68] Mei Z and Chung D D L 2000 Effects of temperature and stress on the interface between concrete and its carbon fiber epoxy-matrix composite retrofit, studied by electrical resistance measurement *Cement Concrete Res.* **30** 799–802
[69] Toutanji H A 1999 Durability characteristics of concrete columns confined with advanced composite materials *Comp. Struct.* **44** 155–61
[70] Toutanji H A and El-Korchi T 1999 Tensile durability of cement-based FRP composite wrapped specimens *J. Comp. Construction* **3** 38–45
[71] Karbhari V M, Engineer M and Eckel D A 1997 II. On the durability of composite rehabilitation schemes for concrete: use of a peel test *J. Mater. Sci.* **32** 147–56
[72] Henkel D P and Wood J D 1991 Monitoring concrete reinforced with bonded surface plates by the acoustic emission method *NDT & E Int.* **24** 259–64
[73] Pandey A K and Diswas M 1994 Damage detection in structures using changes in flexibility *J. Sound Vib.* **169** 3–17
[74] Mei Z and Chung D D L 2000 Kinetics of autohesion of thermoplastic carbon-fiber prepregs *Int. J. Adhesion Adhesives* **20** 173–5
[75] Dixon S, Edwards C and Palmer S B 1994 Analysis of adhesive bonds using electromagnetic acoustic transducers *Ultrasonics* **32** 425–30
[76] Winston V K 1998 Effectiveness of process verification testing to determine quality in commercial aircraft metal bond parts *Proc. 43rd Int. SAMPE Symp. and Exhibition (Covina, CA, SAMPE)* **43** 1428–37
[77] Mei Z and Chung D D L 2000 Thermal stress induced thermoplastic composite debonding, studied by contact

electrical resistance measurement *Int. J. Adhesion Adhesives* **20** 135–9

[78] Mei Z and Chung D D L 2000 Effect of heating time below the melting temperature on polyphenylene sulfide joint development *Int. J. Adhesion Adhesives* **20** 273–7

[79] Luo X and Chung D D L 2000 Interface in mechanically fastened steel joint, studied by contact electrical resistance measurement *J. Mater. Eng. Perf.* **9** 95–7

[80] Luo X and Chung D D L 2001 Degradation of mechanically fastened stainless steel joint during repeated fastening and unfastening *Adv. Eng. Mater.* **3** 62–5

[81] Luo X and Chung D D L 2000 Concrete-concrete pressure contacts under dynamic loading, studied by contact electrical resistance measurement *Cement Concrete Res.* **30** 323–6

[82] Luo X and Chung D D L 2000 Material contacts under cyclic compression, studied in real time by electrical resistance measurement *J. Mater. Sci.* **35** 4795–802

[83] Luo X and Chung D D L 2000 Interface in mechanically fastened polymer joint, studied by contact electrical resistance measurement *Polymer Eng. Sci.* **40** 1505–9